Optical microfiber coil resonator refractometric sensor

Fei Xu, Peter Horak, and Gilberto Brambilla

Optoelectronics Research Centre, University of Southampton, Southampton SO17 1BJ, United Kingdom
fex@orc.soton.ac.uk

Abstract: We present a novel refractometric sensor based on a coated all-coupling optical-fiber-nanowire microcoil resonator which is robust, compact, and comprises an intrinsic fluidic channel. We calculate the device sensitivity and find its dependence on the nanowire diameter and coating thickness. A sensitivity as high as 700 nm/RIU and a refractive index resolution as low as 10^{-10} are predicted.

OCIS codes: (060.2370) Fiber optics sensors; (230.5750) Resonators.

References and links

1. N. M. Hanumegowda, C. J. Stica, B. C. Patel, I. M. White, and X. Fan, "Refractometric sensors based on microsphere resonators," Appl. Phys. Lett. **87**, 201107 (2005).
2. M. Adams, G. A. DeRose, M. Lončar, and A. Scherer, "Lithographically fabricated optical cavities for refractive index sensing," J. Vac. Sci. Technol. B **23**, 3168-3173 (2005).
3. C. Y. Chao, W. Fung, and L. J. Guo, "Polymer microring resonators for biochemical sensing applications," IEEE J. Sel. Top. Quantum Electron. **12**, 134-142 (2006).
4. I. M. White, H. Zhu, J. Suter, N. M. Hanumegowda, H. Oveys, M. Zourob, and X. Fan, "Refractometric sensors for lab-on-a-chip based on optical ring resonators," IEEE Sens. J. **7**, 28-35 (2007).
5. I. M. White, H. Oveys, X. Fan, T. L. Smith, and J. Zhang, "Integrated multiplexed biosensors based on liquid core optical ring resonators and antiresonant reflecting optical waveguides," Appl. Phys. Lett. **89**, 191106 (2006).
6. L. Tong, R. R. Gattass, J. B. Ashcom, S. He, J. Lou, M. Shen, I. Maxwell, and E. Mazur, "Subwavelength-diameter silica wires for low-loss optical wave guiding," Nature **426**, 816-819 (2003).
7. G. Brambilla, V. Finazzi, and D. J. Richardson, "Ultra-low-loss optical fiber nanotapers," Opt. Express **12**, 2258-2263 (2004).
8. S. G. Leon-Saval, T. A. Birks, W. J. Wadsworth, P. St. J. Russell, and M. W. Mason, "Supercontinuum generation in submicron fibre waveguides," Opt. Express **12**, 2864-2869 (2004).
9. M. Sumetsky, "Optical fiber microcoil resonators," Opt. Express **12**, 2303-2316 (2004).
10. M. Sumetsky, Y. Dulashko, J. M. Fini, A. Hale, and D. J. DiGiovanni, "The Microfiber Loop Resonator: Theory, Experiment, and Application," J. Lightwave Technol. **24**, 242-250 (2006).
11. F. Xu and G. Brambilla, "Embedding Optical Microfiber Coil Resonators in Teflon," Opt. Lett. (in press).
12. M. Sumetsky, Y. Dulashko, and M. Fishteyn, "Demonstration of a multi-turn microfiber coil resonator," in *Optical Fiber Communication Conference*, OSA Technical Digest (Optical Society of America, 2007), postdeadline paper PDP46.
13. F. Xu, P. Horak, and G. Brambilla, "Conical and biconical ultra-high-Q optical-fiber nanowire microcoil resonator," Appl. Opt. **46**, 570-573 (2007).
14. F. Xu, P.Horak, and G.Brambilla, "Optimized Design of Microcoil Resonators," J. Lightwave Technol. (in press).
15. D. Marcuse, F. Ladouceur, and J. D. Love, "Vector modes of D-shaped fibers," IEE Proc. J. **139**, 117–126 (1992).
16. M.S. Dinleyici and D.B. Patterson, "Vector modal solution of evanescent coupler," J. Lightwave Technol. **15**, 2316–2324 (1997).
17. C. Y. Chao and L. J. Guo, "Design and Optimization of Microring Resonators in Biochemical Sensing Applications," J. Lightwave Technol. **24**, 1395-1402 (2006).
18. A. N. Chryssis, S. M. Lee, S. B. Lee, S. S. Saini, and M. Dagenais, "High sensitivity evanescent field fiber Bragg grating sensor," IEEE Photon. Technol. Lett. **17**, 1253-1255 (2005).
19. O. Esteban, N. Díaz-Herrera, M.-C. Navarrete, and A. González-Cano, "Surface plasmon resonance sensors based on uniform-waist tapered fibers in a reflective configuration," Appl. Opt. **45**, 7294-7298 (2006).

#82394 - $15.00 USD Received 24 Apr 2007; revised 4 Jun 2007; accepted 5 Jun 2007; published 8 Jun 2007

20. G. M. Hale and M. R. Querry, "Optical Constants of Water in the 200nm to 200m Wavelength Region," Appl. Opt. **12**, 555-563 (1973).
21. M. Cai, O. Painter, and K. J. Vahala, "Observation of critical coupling in a fiber taper to a silica-microsphere whispering-gallery mode system," Phys. Rev. Lett. 85, 74-77 (2000).
22. P. Dress, M. Belz, K. Klein, K. Grattan, and H. Franke, "Physical analysis of teflon coated capillary waveguides," Sens. Actuators B **51**, 278-284 (1998).
23. R. Altkorn, I. Koev, R. P. Duyne, and M. Litorja, "Low-loss liquid-core optical fiber for low-refractive-index liquids: fabrication, characterization, and application in Raman spectroscopy," Appl. Opt. **36**, 8992-8998 (1997).
24. S. Arnold, M. Khoshsima, I. Teraoka, S. Holler, and F. Vollmer, "Shift of whispering-gallery modes in microspheres by protein adsorption," Opt. Lett. **28**, 272-274 (2003).
25. I. Teraoka, S. Arnold, and F. Vollmer, "Perturbation approach to resonance shifts of whispering-gallery modes in a dielectric microsphere as a probe of a surrounding medium," J. Opt. Soc. Am. B **20**, 1937-1946 (2003).
26. S. Campopiano, R. Bernini, L. Zeni, and P. M. Sarro, "Microfluidic sensor based on integrated optical hollow waveguides," Opt. Lett. **29**, 1894-1896 (2004).
27. G. Brambilla, F. Xu, and X. Feng, "Fabrication of optical fibre nanowires and their optical and mechanical. characterisation," Electron. Lett. **42**, 517-519 (2006).
28. F. Prieto, B. Sepúlveda, A. Calle, A. Llobera, C. Domínguez, and L. M. Lechuga, "Integrated Mach-Zehnder interferometer based on ARROW structures for biosensor applications," Sens. Actuators B **92**, 151-158 (2003).
29. F. Prieto, B. Sepúlveda, A. Calle, A. Llobera, C. Domínguez, A. Abad, A. Montoya, and L. M. Lechuga, "An integrated optical interferometric nanodevice based on silicon technology for biosensor applications," Nanotechnology **14**, 907-912 (2003).
30. P. Debackere, S. Scheerlinck, P. Bienstman, and R. Baets, "Surface plasmon interferometer in silicon-on-insulator: novel concept for an integrated biosensor," Opt. Express **14**, 7063-7072 (2006).
31. A. M. Armani and K. J. Vahala, "Heavy water detection using ultra-high-Q microcavities," Opt. Lett. **31**, 1896-1898 (2006).
32. M. L. Gorodetsky, A. A. Savchenkov, and V. S. Ilchenko, "Ultimate Q of optical microsphere resonators," Opt. Lett. **21**, 453-455 (1996).
33. D. W. Vernooy, V. S. Ilchenko, H. Mabuchi, E. W. Streed, and H. J. Kimble, "High-Q measurements of fused-silica microspheres in the near infrared," Opt. Lett. **23**, 247-249 (1998).
34. K. J. Vahala, "Optical microcavities," Nature **424**, 839-846 (2003).
35. D. K. Armani, T. J. Kippenberg, S. M. Spillane, and K. J. Vahala, "Ultra-high-Q toroid microcavity on a chip," Nature **421**, 925-928 (2003).
36. B. S. Song, S. Noda, T. Asano, and Y. Akahane, "Ultra-high-Q photonic double-heterostructure nanocavity," Nature Mater. **4,** 207-210 (2005).

1. Introduction

In the past few years, evanescent-field-based optical resonators in the form of microspheres, photonic crystals, and microrings have been under intensive investigation for deployment as biological and/or chemical sensors [1-5]. For these applications, small size, high sensitivity, high selectivity, and low detection limits are the dominant requirements. Optical microresonators meet all these criteria, in particular they can provide large evanescent fields for high sensitivity, high Q-factors for low detection limits, and corresponding small resonant bandwidths for good wavelength selectivity. The drawback that all high-Q resonators present relates to the difficulty of coupling light into and out of the resonator. Following a fast development of fabrication technology in recent years, subwavelength-diameter optical nanowires have emerged as an ideal sensor element because of low cost, low loss, and very large evanescent fields [6-8]. Moreover, self-coupling of optical nanowires can be exploited in high-Q microresonators such as loops or 3D microcoils [9, 10]. These fiber microresonators do not exhibit the input/output coupling problems experienced in other high-Q resonators because the fiber pigtails at the extremities of the resonator launch and collect the totality of the light. However, in free space the fabrication of these devices with high reliability is challenging due to problems of stability, degradation, and cleanness. Coating is an elegant way to solve these issues. Recently, 3D microcoil resonators were experimentally demonstrated in Teflon [11] and in low index liquid [12]. Here we analyze a refractometric sensor based on a coated optical nanowire microcoil resonator and investigate its performance

#82394 - $15.00 USD Received 24 Apr 2007; revised 4 Jun 2007; accepted 5 Jun 2007; published 8 Jun 2007

as a function of the geometry, in particular, the nanowire diameter and the coating thickness. Both parameters need to be optimized to obtain a strong and compact device with a significant fraction of optical power propagating in the evanescent field inside the fluidic channel. We show that high sensitivity and ultra-low detection limits are feasible with such a device.

2. Fabrication

A coated all-coupling nanowire microcoil resonator (CANMR) can be fabricated as follows [11]. First, an expendable rod is initially coated with a layer of thickness *d* of a low-loss polymer such as Teflon. Then an optical fiber nanowire is wrapped on the rod. Next, the whole structure is coated with the same low-loss polymer, and finally the rod is removed. Figure 1 shows the final structure after the rod is removed: the nanowire is shown in blue, the analyte channel (in the space previously belonging to the rod) in grey and Teflon in green. It is a compact and robust device with an intrinsic fluidic channel to deliver samples to the sensor, unlike most ring or microsphere resonators which require an additional channel. The embedded nanowire has a considerable fraction of its mode propagating in the fluidic channel, thus any change in the analyte properties reflects in a change of the mode properties at the CANMR output. Since the CANMR is fabricated from a single tapered optical fiber, light can be coupled into the sensor with essentially no insertion loss, a huge advantage over other types of resonator sensors. Self-coupling of the nanowire can be optimized by various methods to form a high Q-factor resonator [13, 14].

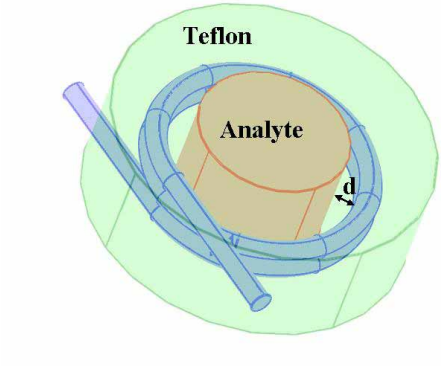

Fig. 1. Schematic of the CANMR.

3. Theory of the CANMR

Assuming continuous-wave (cw) input, a change of the analyte refractive index will lead to a change of the effective index n_{eff} of the propagating mode, thereby shifting the mode relative to the resonance and thus modifying the transmission coefficient *T*. In this paper, we only investigate the simplest case of a two-turn resonator, which can be easily extended to the case of multi-turn resonators. A two-turn CANMR can be easily evaluated using coupled mode equations with results analogous to those of a single-loop resonator [10]; if $\beta = 2\pi n_{eff}/\lambda$ is the propagation constant, α the loss coefficient, and $K = \kappa L$ the coupling parameter for coupling coefficient κ and nanowire length *L* of a single turn, then *T* can be written as [9]:

$$T = \frac{\exp(i\beta L - \alpha L) - i\sin K}{\exp(-i\beta L + \alpha L) + i\sin K}. \quad (1)$$

Resonances in *T* occur if *K* and β are near to values

$$K_m = \arcsin\gamma + 2m\pi, \quad (2)$$

$$\beta_n = (2n+1)\pi/(2L), \quad (3)$$

#82394 - $15.00 USD Received 24 Apr 2007; revised 4 Jun 2007; accepted 5 Jun 2007; published 8 Jun 2007

respectively, where $\gamma = \exp(-\alpha L)$ and m and n are integer numbers.

Because of the interface with the analyte, the mode propagating in the coated fiber nanowire experiences a refractive index surrounding similar to that of a conventional D-shaped fiber [15, 16]. The mode properties are particularly affected by two important parameters: the nanowire radius r and the coating thickness d between the nanowire and the fluidic channel. We evaluated the effective index n_{eff} of the fundamental mode propagating in the optical fiber nanowire by a finite element method with the commercial software COMSOL3.3. Figure 2 shows the dependence of n_{eff} on the analyte refractive index n_a assuming the refractive index of the nanowire and of Teflon to be n_c=1.451 and n_t=1.311, respectively. Here we use the parameters r=500 nm and the three values 10 nm, 100 nm, and 500 nm for d. The fundamental mode is the one with the largest propagation constant and the only mode that is well confined in the vicinity of the nanowire [16]. Generally, n_{eff} increases with n_a, and increases more quickly with smaller d since in this case a larger fraction of the mode is propagating in the analyte. If n_a=n_t, light cannot see the boundary between Teflon and the analyte solution, and therefore n_{eff} is independent of the Teflon thickness d, as seen in Fig. 2.

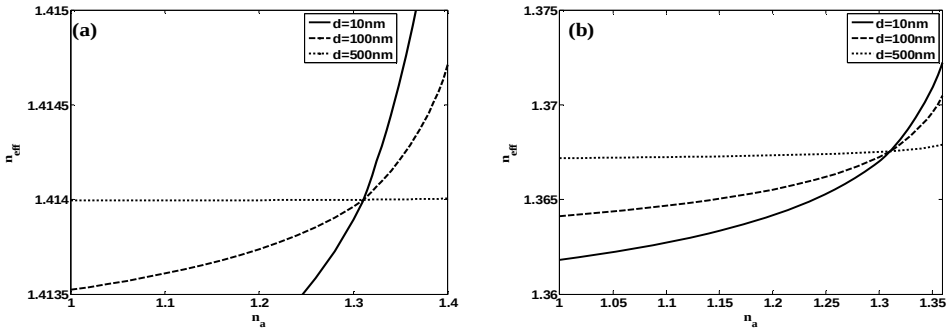

Fig. 2. Dependence of the effective index of a coated nanowire n_{eff} on the index of the analyte n_a for n_t=1.311, n_c=1.451, r=500 nm, d=10 nm (solid line), 100 nm (dashed), and 500 nm (dotted). The wavelength of the propagating mode is (a) λ=600 nm, (b) λ=970 nm.

4. Sensitivity and detection limit

Two sensing approaches are most commonly used: homogeneous sensing and surface sensing [17]. In homogeneous sensing, the device is typically surrounded by an analyte solution, which can be regarded as the top cladding of the waveguide. The homogeneously distributed analyte in the solution will modify the bulk refractive index of the solution. In surface sensing, the optical device is pretreated to have receptors or binding sites on the sensor surfaces, which can selectively bind the specific analyte [17]. Here we only discuss the conceptually simpler case of homogeneous sensing.

The homogeneous sensitivity S obtained by monitoring the shift of the resonant wavelength λ_0 corresponding to one of the propagation constants β_n (3) can be defined as [17]

$$S = \frac{\partial \lambda_0}{\partial n_a} = \frac{\partial \lambda_0}{\partial n_{eff}} \frac{\partial n_{eff}}{\partial n_a} = \frac{\lambda_0}{n_{eff}} \frac{\partial n_{eff}}{\partial n_a} \tag{4}$$

Because water is the solvent for most analytes and the absorption of water at long wavelengths is high [20], we calculated the sensitivity near n_a=1.332 at short wavelengths (600 nm and 970 nm). Figure 3 shows the dependence of S on the nanowire radius r for different d. S increases when d decreases or λ increases in accordance with the results of Fig. 2. Decreasing the nanowire radius r also increases sensitivity because this increases the fraction of the mode field inside the fluidic channel. S reaches 500 nm/RIU (where RIU is refractive index unit) at r≈200 nm for λ=600 nm and 700 nm/RIU at r≈300 nm for λ=970 nm.

#82394 - $15.00 USD Received 24 Apr 2007; revised 4 Jun 2007; accepted 5 Jun 2007; published 8 Jun 2007

This is higher than in most microresonator sensors [1, 4]. For even smaller values of *r*, the fundamental mode is no longer well confined and propagation losses become so large that they prevent the operation of the sensor in this regime.

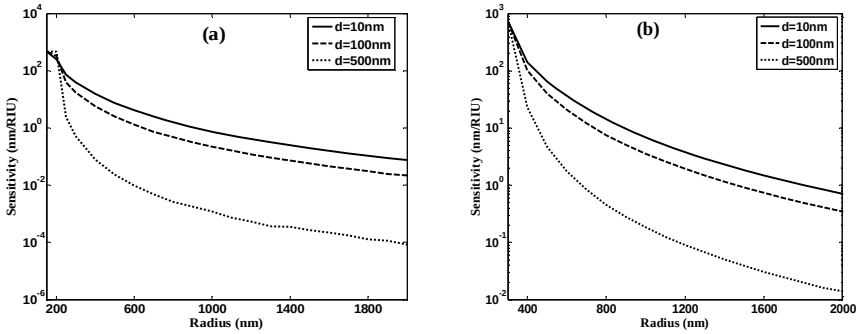

Fig. 3. Sensitivity of the CANMR versus nanowire radius for (a) λ=600 nm and (b) λ=970 nm and for different values of *d*. Here, n_a=1.332, n_t= 1.311, and n_c=1.451.

For a resonator wavelength-shift sensor, the detection limit (defined as the smallest detectable refractive index change of analyte) is another critical parameter to evaluate the sensing capability of a device. The detection limit can be defined as $\delta\lambda_0/S$, where $\delta\lambda_0$ is the smallest measureable wavelength shift. Generally, $\delta\lambda_0$ is limited by instrument resolution and is assumed as 1/20 of the full width at half maximum (FWHM) of the monitored resonance [1]. Table 1 summarizes the features of the most common evanescent field sensors as reported in the literature. For grating and plasmon-resonance sensors, sensitivities can be as high as 10000 nm/RIU [18, 19], but because of a very large bandwidth (>0.1 nm) the detection limit is restricted.

For the CANMR, the FWHM and Q-factor depend on the resonator coupling and loss. For resonant coupling, $K=K_m$, cf. Eq. (2),

$$FWHM = \frac{\lambda_0^2}{\pi n_{eff} L}\left|\frac{\pi}{2} - \arcsin\left[\frac{\left(\gamma^2+\gamma^{-2}\right)}{2\left(\gamma^2+\gamma^{-2}\right)-2}\right]\right| \approx \frac{\lambda_0^2}{\pi n_{eff} L}\sqrt{\frac{\left(\gamma^2+\gamma^{-2}\right)-2}{\left(\gamma^2+\gamma^{-2}\right)-1}} \approx \frac{2\lambda_0^2\alpha}{\pi n_{eff}} \tag{5}$$

and for near-resonant coupling

$$FWHM \propto \alpha + (K-K_m)^2 \tag{6}$$

which is independent on *L*, thus the detect limitation is also independent on *L*.

In traditional microresonators light is coupled into the resonator using prism coupling, anti-resonator reflecting waveguide coupling, or fiber taper coupling [1-5]. With probably the only exception of the fiber taper coupling, which has been proved to be reasonably efficient [21], coupling to microresonator has been considerably complicate in terms of device design and/or of increase of the overall loss. The CANMR, on the other hand, has low insertion loss. Resonant coupling and therefore high Q-factors can also be achieved by optimized designs [13, 14]. Losses in the CANMR arise from surface scattering, material (analyte, coating, and fiber) absorption, and bending of coils. The smallest reported loss of an optical nanowire is about α=0.001 dB/mm with radii in the range of hundreds of nanometers [8, 25]. The water absorption can be reduced to levels well below 0.0001 dB/mm by operating at short wavelengths [20]. Cladding materials (such as Teflon or UV375) can be used for low coating loss. For example, for water-core Teflon waveguides losses of 1 dB/m have been reported [22, 23]. The estimated bend loss [9] for a 200-nm-radius nanowire and a 500-μm-diameter coil at a wavelength of 600 nm is 0.0001 dB/mm, which quickly decreases further with increasing

#82394 - $15.00 USD Received 24 Apr 2007; revised 4 Jun 2007; accepted 5 Jun 2007; published 8 Jun 2007

coil diameters. Therefore, if we assume α=0.01 dB/mm, the other losses can be neglected and for a CANMR with r=200 nm at λ=600 nm, the FWHM is 4×10^{-7} nm and the detection limit is 10^{-10}-10^{-11} RIU, which is lower than any reported experimental result or theoretical prediction [24, 25]. We note that microresonators with extremely high Q-factor have been demonstrated in particular with microspheres and microrings [31-36], which upon optimization could lead to sensitivities comparable to the one predicted for the CANMR here. However, the ease of mode size control via the nanowire diameter and the lossless input and output coupling via the fiber pigtails are unique features of the CANMR. Additionally, planar ring resonators are expected to have similar sensitivities when similar design parameters are used. Yet, from the experimental point of view it is extremely challenging to achieve losses comparable to the loss achieved in microfibers.

Table 1. Summary of sensitivity and FWHM for evanescent field refractometric sensors.

Type of sensor	$\delta\lambda/\delta n$ (nm/RIU)	λ (nm)	FWHM (nm)	FWHM/ $\delta\lambda/\delta n$ (RIU)	Ref.
Microsphere	30	980	$2\cdot10^{-4}$	$6\cdot10^{-6}$	[1]
Photonic crystal microresonator	228	1500	~1	$3\cdot10^{-3}$	[2]
Microcapillary	45	980	$1.55\cdot10^{-4}$	$3\cdot10^{-6}$	[4]
Grating	1000	1550	>0.1	10^{-5}	[18]
Surface Plasmon Resonance	10000	850	>1	10^{-5}	[19]
Hollow-core ARROW*	555	700	>1	$2\cdot10^{-3}$	[26]
Mach – Zehnder Interferometry-ARROW*				$7\cdot10^{-6}$	[28]
Mach – Zehnder Interferometry-TIR**				$2\cdot10^{-5}$	[29]
Surface Plasmon				10^{-6}	[30]
CANMR	700	970	$<4\cdot10^{-7}$	10^{-10}	**This work**

* ARROW (Anti Resonant Reflecting Optical Waveguides). ** TIR (Total Internal Reflection).

5. Conclusion

In summary, we have investigated a novel refractometric sensor in the form of a coated all-coupling nanowire microcoil resonator, which is strong, extremely compact, and has an intrinsic fluidic channel. For optimized designs, sensitivities up to 700 nm/RIU can be achieved. Detection limits of the order of 10^{-10} have also been predicted. Compared to other microresonator sensors, this novel device has potentially the largest Q-factor and the lowest detection limit.

Acknowledgments

The authors gratefully acknowledge the help of Dr. N. Broderick with the software package COMSOL, initiating discussions with Prof. D. J. Richardson, and financial support by the EPSRC under the standard research grant EP/C00504X/1.

#82394 - $15.00 USD Received 24 Apr 2007; revised 4 Jun 2007; accepted 5 Jun 2007; published 8 Jun 2007